Minimax Theory and its Applications

Volume 11 (2026), No. 5s, 273-281

Modelling and Interpretation of Brown-Bear Optimization with Hybrid Deep Learning based Scheduling Approach for Urban Drainage Networks

J. Suganthi[1]*, I. Paulraj Jayasimman[2]

[1]Research scholar, Academy of Maritime Education and Training (AMET), Deemed to be University, India, Email: sugisuresh27@yahoo.in

[2]Associate Professor, Department of Mathematics, Academy of Maritime Education and Training (AMET), Deemed to be University, India, Email: ipjayasimman@ametuniv.ac.in

*Corresponding Author

Abstract

Urban drainage networks (UDNs) are applied in the urban framework to drain rainwater and/or utilized water from the model, which has not caused floods. Accordingly, higher-dimensional replications for UDN modeling are usually accomplished, and two-dimensional (2D) hydraulic/hydrodynamic statistical must be considered. 2D methods have been extensively applied to calculate composite flood-inundation dynamics and hydrological procedures. In recent times, deep learning (DL) techniques have proven to the possible to be used and applied in UDNs because of their capability to deal with issues in different science or engineering fields. Effective drainage not only strengthens the framework, like sewage and rain change, drainage and storage, pollution source monitoring, transportation, but also immediately requires technical means to optimize and monitor operation and production. This study develops an optimal deep learning-based scheduling approach for UDNs, named the ODLSA-UDN technique. The proposed ODLSA-UDN technique is intended for the optimum control of a 1-stage pumping station and the synchronized control among 2-stage pumping stations. Besides, the ODLSA-UDN technique applies a squeeze-and-excitation block with a fully convolutional network (SE-FCN) water level prediction method of the sewage pumping places, and then, depending on the mechanism of the drainage pipeline system analysis, the reasons that can lead to the water level change of the pumping station are gained. Moreover, the parameter fine-tuning of the SE-FCN model takes place utilizing the brown-bear optimization algorithm (BBOA). Grey correlation analysis is performed on these key factors, and the prediction method is recognized by considering the factors with a higher correlation amount as input. The experimental outcomes indicate that compared to the conventional prediction method, the proposed method not only has greater prediction precision but also has improved inflection point tracking capability.

Keywords—Urban drainage networks; Grey correlation analysis; Deep learning; Pumping station; Squeeze-and-excitation

Introduction

The urban drainage system (UDS) is a vital component of urban infrastructure, serving to maintain environmental sanitation, improve living standards, mitigate water-related hazards, and enhance the effectiveness of water resource management [1]. Currently, the growth of the Internet of Things (IoTs) has allowed gathering, transferring, analyzing, and utilizing data, and has significantly advanced the growth of UDS by facilitating real-time monitoring and efficient management of water flow [2]. Extensive drainage monitoring data has facilitated the advancement of intelligent water management systems. The use of sophisticated information technology, namely big data analytics and artificial intelligence (AI), in the setting of smart water management allows drainage monitoring data processing and analysis, resulting in the automated and optimized management and control of drainage systems [3]. This results in improved water resource management and better-informed decisions by water authorities. Data analysis is crucial for detecting the in-built patterns in the observed data, which, in turn, highlights the need for higher-quality drainage data [4]. High-quality drainage data can deliver precise data, assist efficient planning and management, and be utilized for predicting future

needs and difficulties for the system [5]. As a vital constituent of the smart water development, extensive drainage observing data is needed to confirm the accuracy of the model in real-time scenarios [6]. Nevertheless, real-time monitoring data frequently comprises several irregular values, which can significantly influence the data analysis and modelling outcomes [7]. Fig. 1 depicts the general structure of urban drainage systems.

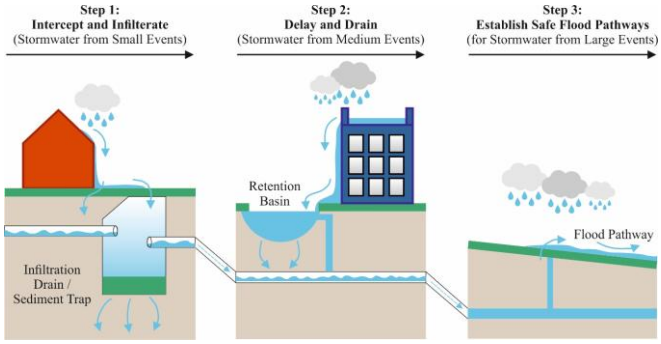

Fig. 1. General Structure of urban drainage system

However, the function assessments in several UDS issues, for example, real-time operation control, and flood-inundation forecasting, are normally carried out through 2D, which demands higher computational power due to the simulation time involved for rainfall-runoff and pipe network hydraulics [8]. This important constraint can be solved with the help of machine learning (ML) techniques [9]. ML is fundamentally reshaping our world, industries, and scientific and technical fields. ML allows machines to learn from data without being explicitly programmed, but with inferences and patterns acquired from data [10]. At present, ML techniques, such as classification, regression, and clustering, are being swapped with novel ML techniques, like deep learning (DL) [11].

This article develops an optimum DL-based scheduling technique for UDNs, named ODLSA-UDN system. Furthermore, the ODLSA-UDN method uses a squeeze-and-excitation block with a fully convolutional network (SE-FCN) water level prediction technique of the sewage pumping regions, and then relies on the method of drainage pipeline system analysis. The brown-bear optimization algorithm (BBOA) is used for a parameter tuning approach. Grey correlation analysis is executed on these main factors, and the prediction technique is detected by considering the factors with an advanced correlation amount as input. The experimental outcomes indicate that compared to the conventional prediction method, the proposed method not only has greater prediction precision but also has improved inflection point tracking capability.

Literature Survey on Urban Drainage Networks

D'Souza et al. [12] introduced a Solar-Powered Autonomous Road Cleaning Robot that utilizes solar energy, IoT monitoring, and AI-based navigation. In a small, rust-resistant chassis, the robot has dual rotating brushes, a retractable drainage cleaning pipe, and a vacuum system. The AI path planning enables autonomous navigation and identifies hurdles instantly. The IoT integrations assist in tracking and monitoring the robot and can also collect data automatically. Solar consumption optimizes energy sustainability in high cleaning, drainage maintenance, and navigation. In [13], a digital twin experimental stage for lake and river water systems has been designed to improve the inclusive urban flood control and drainage management. This stage incorporates a backend system, an engineering entity, and a digital twin module. Virtual-real interactions and real-time data acquisition among physical facilities and the digital twin are attained through the PLC technique, whereas the Unity3-D engine facilitated sophisticated visualization and data rendering.

Cai et al. [14] introduced a MDPIS technique as an active solution to address urban flooding using the drainage system discharge capabilities optimization. This technique's strength is confirmed by the incorporation of a multi-tier drainage network and dependence relations. Moreover, the combination of a significant parameter is taken into account for enabling real-time examination of the flooding risk assessment. This technique was utilized for simulating a drainage system, and the outcomes specify that its precision, reliability, and adaptability surpass those of current systems, namely fixed-priority scheduling. Situ et al. [15] presented a new attention-based DL system for refining urban flood risk evaluation using vulnerability assessment. Afterward, the ES-DeepLab segmentation approach is presented by merging squeeze-and-excitation (SE) and EfficientNet-Lite4 mechanisms that enhanced computational precision and efficacy in fine-grained land use classification.

You-Fei et al. [16] introduced a FNN control architecture depending on diverse working conditions to enhance the entire procedure of municipal sewage sludge treatment and discharge. This architecture initially splits the working conditions based on the weather, creating distinct features and input vectors. Next, the FNN has been utilized to achieve the control and optimization of several indicators, attaining the dual aims of decreasing

energy consumption and optimizing water quality. Sun et al. [17] suggested the detention tank draining time as a fresh reliability assessment indicator that significantly decreases the calculation problem by transforming the risk of water quality into the risk of hydraulic. Based on this, rainfall effects, actuators, dry weather flow (DWF), and their connections on reliability are measured.

Methodological Framework

In this manuscript, we develop an optimum DL-based scheduling technique for UDNs, named ODLSA-UDN system. The presented ODLSA-UDN system is intended for the optimum control of the 1st-stage pumping station and the synchronized control between second-stage pumping stations. It contains water level prediction, parameter tuning, and grey correlation analysis. Fig. 2 represents the entire workflow of the ODLSA-UDN system.

SE-FCN-based Water Level Prediction Technique

In addition, the ODLSA-UDN technique applied the SE-FCN water level prediction technique to the sewage pumping areas. The SE blocks the interdependencies among the feature mapping channels, and perform the process of spatial squeeze in addition to the process of channel excitation [18]. The squeeze process creates channel-wise information that characterizes global data of all channels in feature mapping by utilizing global average pooling. The convolution networking function as:

$$u_c = v_c^{\star} X \qquad (1)$$

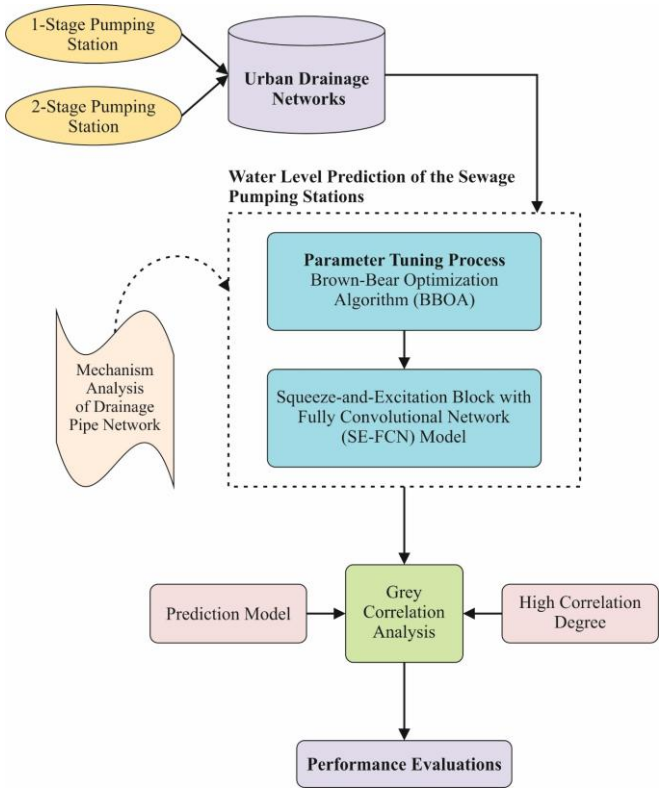

Fig. 2. Entire Work Flow of ODLSA-UDN System

Now, u_c signifies the outputs as $U = [u_1, u_2, \cdots, u_c], v_c$ refers to the spatial kernel as $v_c = [v_c^1, v_c^2, \ldots, v_c^{c'}], X$ specifies the inputs as $X = [x^1, x^2, \ldots, x^{c'}]$, and $*$ signifies the convolution.

In segmentation, the squeeze function is expressed as shown:

$$z_c = F_{sq}(u_c) = \frac{1}{H \times W} \sum_{i=1}^{H} \sum_{j=1}^{W} u_c(i, j) \qquad (2)$$

Whereas z_c stands for cth component of the squeezed channels, u_c indicate cth component of the input, and F_{sq} Indicate the squeeze function that provides a vector. W and H represent the width and height of input, respectively.

The excitation process comprises ReLU(rectified linear unit) and the fully connected (FC) layers to adaptively strengthen informative features and overwhelm the minimum valuable one, which specifies that the SE block refers to self-gating mechanism.

$$s = F_{ex}(z, W) = \sigma\big(W_2\delta(W_1 z)\big) \tag{3}$$

Here, F_{ex} symbolize an excitation function that can be parameterized by 2-layer FC neural networks (NNs). z means input squeezed descriptor from the preceding layer. σ specifies a function of sigmoid, and δ denotes ReLU. W_1 and W_2 represent the 1x1 convolutional layers. W_1 refers to dimensionality reduction using the parameter reduction ratio r, and W_2 refers to improving dimensionality. Values of s are within the range of zero and one. The network's last output is computed by converting the output size.

$$\tilde{x}_c = F_{scale}(u_c, s_c) = s_c \cdot u_c \tag{4}$$

Now, F_{scale} specifies a rescaling function that signifies channel-by-channel multiplication among the scalars s_c and the feature maps u_c.

The FCN (fully convolutional neural network) includes various layers of the output layer and elementary convolutional blocks, while all convolutional blocks have the responsibility to remove feature data at various levels [19]. The resultant layer utilizes an 1x1 convolution kernel to attain feature mapping and channel compression to create the last prediction outcomes. In comparison with the classic layer of fully connected (FC), the convolution process of FCN not only lowers the parameter counts but also maintains the spatial data that is beneficial to capture the local attributes of the input information. In the meantime, its flexibility enables it to perform well in the task's diversity, particularly after addressing larger-scale data. It can tune and recombine features at various levels, also improving the generalizability of the method. This design approach allows the DL method to adjust well to different input information, guaranteeing precision and reliability in practical use. Every convolutional block includes a 1D convolutional layer, an activation function, and batch normalization (BN). Next, the convolutional layer output is fine-tuned utilizing normalization methods to maintain the data distribution output steady to speed up convergence of the model and increase training outcomes. Eventually, the non-linear attributes are presented by changing the linear unit (ReLU) to increase the expression capability of the non-linear issue. The 1D convolutional formulation is as demonstrated:

$$e_{j,t} = w_b + \sum_{t'=1}^{d} w_{j,t'}\, x_{j,t+t'} \tag{5}$$

Whereas $x_{j,t}$ represent the input feature j at moment t, $e_{j,t}$ refers to the output feature j within the layer of convolutional at moment t, $w_{j,t'}$ characterizes the equivalent tensor weighting of feature j, and w_b means the convolution biased term. The convolution kernel dimensions d fix the perceptual field range of the convolution network.

$$u_j = \frac{1}{T}\sum_{t=1}^{T} e_{j,t} \tag{6}$$

$$\sigma_j^2 = \frac{1}{T}\sum_{t=1}^{T} (e_{j,t} - u_j)^2 \tag{7}$$

$$e_{j,t} = \gamma \frac{e_{j,t} - \mu_j}{\sqrt{\sigma_j^2 + \varepsilon}} + \beta \tag{8}$$

Whereas u_j and σ_j^2 specifies the mean and variance of feature j, $e_{j,t}$ Signifies the matrix after standardization, γ denotes the scaling parameter applied to fine-tune the variance in the normalization procedure, β denotes the biased term applied to implement the translation after standardization, and ε indicates the minimum constant presented to avoid the error of dividing by 0. These constraints work together to guarantee that the method is steady sufficient for learning the distribution of dissimilar attributes in the training procedure, preventing the problem of vanishing or gradient explosion and increasing the training efficacy and model's performance. The Leaky ReLU's activation function equation is as demonstrated:

$$y_{j,t} = f(\hat{e}_{j,t}) = \max(0, \hat{e}_{j,t}) + \alpha * \min(0, \hat{e}_{j,t}) \tag{9}$$

In the architecture of SE-FCN, SE blocks are tactically embedded after the main convolutional layers inside the decoder and/or encoder steps of the FCN. This incorporation presents a channel-wise attention mechanism that improves the ability of the model to underline important features while suppressing less informative ones. By recalibrating the learned feature maps, the SE block increases the sensitivity of the network to contextually important information and lowers the influence of irrelevant channels or background noise. The recalibrated output feature maps Y' in the SE-FCN are mathematically expressed as:

$$Y' = \mathrm{SEBlock}\big(\mathrm{Conv}(X)\big) \quad (10)$$

Now, X denotes the input feature map, Conv represents the convolutional operation, and $\mathrm{SEBlock}$ uses global feature squeezing accompanied by excitation to reweight the channels dynamically.

Parameter Tuning using BBOA Method

Moreover, the parameter tuning of the SE-FCN approach occurs using BBOA. BBOA simulates the foraging behavior of brown bears, their adaptability to the environment, and their evolving search strategies [20]. Predominantly observed in male bears, pedal scent marking serves as a primary mode of interaction. In BBOA, this pedal marking and associated sniffing behavior enhance the algorithm's exploration capabilities within the search space. The territory marking features aid in accomplishing a greater balance between exploitation and exploration, therefore allowing BBOA to manage intricate concerns. The exploration and exploitation stages are described as dual, different entities in BBOA, inducing an enhanced searching mechanism as a dynamic condition of input. But in PSO, either two stages were intertwined together inducing a likelihood of falling into local optima.

The following stages are the hyperparameter tuning process:

1. Initializing parameters: Maximal iteration counts $-G_{max}$, Size of population-pop, Dimension-D, Range for parameters. The hyperparameter for RF methodology has been deliberated as estimator counts, minimal samples, and maximal depth.

2. Set existing iteration, $g = 1$, and calculate FF, MSE(X) for initial population, where X depicts every set of hyper-parameters from the population. MSE is calculated once the method is trained with the primary value of the parameters.

3. Choosing the finest FF (MSE_{best}) and the equivalent hyperparameters (X_{best}).

4. Calculate (P^g, Q^g, S^g, ω^g) utilizing the Eqs. (11) to (14).

$$P^g = \frac{g}{G_{max}} \quad (11)$$

$$Q^g = rand_q . P^g \quad (12)$$

$$S^g = round(1 + rand_s) \quad (13)$$

$$\omega^g = 2 . P^g . \pi . rand_t \quad (14)$$

Here Q^g depicts a factor step, S^g signifies the length of a step, P^g denotes the factor of occurrence, $rand_q$, $rand_s$and $rand_t$ represents random numbers distributed equally among zero and one, ω^g refers to the angular velocity of foot twisting, equivalent to g^{th} iteration .

5. Set the population with the worst fitness as X_{worst} and best fitness as X_{best}.

Exploitation stage

For each member in the set of population, execute steps 6-8 iteratively.

6. Upgrading the pedal differentiation, X_j^{new} of jth group of brown bears utilizing Eqs. (15)-(17) based on the values of P^gThe factor of existence. Eq. (15) indicates gait, whereas walking, Eq. (16) depicts the careful stepping feature of bears, and Eq. (17) denotes the characteristic named twisting of feet.

$$X_j^{new} = \left\{X_j^g - (P^g . rand_\omega . X_i^g)\right\}, \text{if } P^g > 0 \text{ and } P^g < \frac{1}{3} \quad (15)$$

$$X_j^{new} = \{X_j^g + Q^g.\left(X_{Best}^g - S^g.X_{Worst}^g\right\}, \text{if } P^g > \frac{1}{3} \text{ and } P^g < \frac{2}{3} \quad (16)$$

$$X_j^{new} = \left\{X_j^g + \omega^g.\left(X_{Best}^g - |X_j^g|\right) - \omega^g.(X_{Worst}^g + |X_j^g|\right\}, \text{if } P^g > \frac{2}{3} \quad (17)$$

Now X_{Worst}^g and X_{Best}^g and depicts the worst and best pedal differentiations at g^{th} iteration and X_j^g refers to the existing pedal differentiation of jth A group of brown bears at g^{th} iteration.

7. Calculate fitness evaluation, MSE (X_j^{new}) for the novel upgraded parameters, X_j^{new}.

8. Upgrading the hyperparameter set, X_j^g equivalent to the gth iteration and its FF, MSE (X_j^g), only if Eq. (18) is fulfilled. Then, there will not be any update for the parameter set, j.

$$\text{MSE}\left(X_j^{neiv}\right) < \text{MSE}\left(X_j^g\right) \quad (18)$$

Exploration stage

9. Selecting an arbitrary set of hyperparameters(X_k^g) in the population and relate its MSE (X_k^g) value with each other's solution.

10. Evaluating the parameters (X_j^{new}) and its FF, MSE(X_j^{new}utilizing in Eq. (19)

$$X_j^{new} = \begin{cases} X_j^g + \text{rand}_n.\left(X_j^g - X_k^g\right), \text{if MSE}\left(X_j^g\right) < \text{MSE}\left(X_k^g\right) \\ X_j^g + \text{rand}_n.\left(X_k^g - X_j^g\right), \text{otherwise} \end{cases} \quad (19)$$

Now $\text{MSE}(X_j^g)$ and $\text{MSE}(X_k^g)$ refers to the values of FF for the jth and k^{th} A group of brown bears at g^{th} iteration.

11. Upgrade the parameters (X_j^g) and its FF, MSE (X_j^g), only if Eq. (18) is fulfilled.

12. Endure from step 4 to 11 still the convergence conditions are obtained.

13. Test the ML technique with the last set of parameters and assess the performance metrics.

Grey Correlation Analysis

Grey correlation analysis is implemented on these main factors, and the prediction technique is identified by considering the factors with the maximum correlation amount as input. Gray correlation designates the uncertain correlation between things or factors, or system factors, on the major behavior [21]. This model performs the analysis based on the developing tendency of things for that there is limited need for the sample size volume, and there do not demand for a characteristic distribution law, and the calculation volume is comparatively smaller, and the outcomes should also be equivalent with the outcomes of the qualitative study, therefore, this model is an identical with its singular benefits, more reliable and practical method of analysis.

They discovered a new technique to predict security by combining TabNet, a DL structure for tabular data using gray relational analysis (GRA). This incorporation offers a predictive technique that procedures recognition data and computes complete values, enhancing decision-making for security evaluation. The major stages are (1) utilizing gray correlation analysis for assigning weights to indicators; (2) computing the complete value.

Initially, get the comparison vector and reference vector, and consider the reference vector. $x_1 = \{x_1(1), x_1(2), \cdots x_1(n)\}$, n denote sample counts. The comparison vector $x_i = \{x_i(1), x_i(2), \cdots x_i(n)\}, i = 1,2, \cdots, m, m$ represent indicator counts. Normalizing the data based on the average of the finding outcomes of all indicators to remove the effect of the scale, and Eq. (20) is as demonstrated:

$$f_j(k) = \frac{x_j(k)}{\frac{1}{n}\sum_{m-1}^{n} x_j(m)} \quad (20)$$

Subsequently, the correlation coefficients are computed, and the gray correlation coefficients (GCC) of $f_1(k)$ and $f_j(k)$ At the moment k is presented in Eq. (21):

$$\xi_j(k) = \frac{\min_j \min_k \left|f_1(k) - f_j(k)\right| + \rho \max_i \max_{k|f_1(k)-f_j(k)|}}{\left|f_1(k) - f_j(k)\right| + \rho \max_j \max_k \left|f_1(k) - f_j(k)\right|} \quad (21)$$

In Eq. (21): $\xi_j(k)$ indicate GCC; ρ means adjustment parameter that may make the coefficients more distinguished, now ρ is considered as 0.5.

The coefficients of association among orders are provided in Eq. (22):

$$y(f_1, f_j) = \frac{1}{n}\sum_{k=1}^{n}(k) \quad (22)$$

To guarantee the precision of the outcomes, every indicator has been applied to perform as a reference order, then the correlation coefficients matrix for every indicator is gained, as revealed in Eq. (23):

$$y = \begin{bmatrix} y_{11} & y_{12} & \cdots & y_{1m} \\ y_{21} & y_{22} & \cdots & y_{2m} \\ \vdots & \vdots & \ddots & \vdots \\ y_{m1} & y_{m2} & \cdots & y_{mm} \end{bmatrix} \quad (23)$$

According to the gained matrix of GCC, the weighted vector is computed as characterized in Eq. (24):

$$W = \frac{1}{m}\sum_{i=1}^{m}\frac{y_{ij}}{\sum_{j=1}^{m} y_{ij}} \quad (24)$$

Here, m denotes indicator counts; y_{ij} indicate the GCC among the indicators in column j and row i of the matrix.

Then, it is essential to compute the value of complex evaluation that is needed to be dimensionless, particularly, the ratio of the factor's actual recognized value to the limited value of key metrics of the indicator, a, as displayed in Eq. (25):

$$P_{ij} = \frac{x_{ij}}{a_j} \quad (25)$$

Now, P_{ij} stands for the value of relative gain by dimensionless quantization of the ith testing outcome x_{ij} of the jth factor, while, $i = 1,2,\cdots,n, j = 1,2,\cdots,m$; a_j denote the normal limited value of indicator of the initial factor.

Multiplying the weighted vector gained from Eq. (24) using the comparative matrix of all indicators gained in Eq. (25), the complete evaluation order is gained as in Eq. (26).

$$Y = \begin{bmatrix} y_1 \\ y_2 \\ \vdots \\ y_n \end{bmatrix} = P \times W = \begin{bmatrix} p_{11} & p_{12} & \cdots & p_{1m} \\ p_{21} & p_{22} & \cdots & p_{2m} \\ \vdots & \vdots & \ddots & \vdots \\ p_{n1} & p_{n2} & \cdots & p_{nm} \end{bmatrix} \begin{bmatrix} w_1 \\ w_2 \\ \vdots \\ w_m \end{bmatrix} \quad (26)$$

Whereas $Y = y_1, y_2, \cdots, y_n]^T$ refers to sequence of complete evaluation; P indicate relative matrix; and $W = [w_1, w_2, \cdots, w_m]^T$ signifies weight vector. At this stage, the preferred output labels of the method can be calculated.

Experimental Results and Discussion

The performance analysis of the ODLSA-UDN model is examined.

Table 1 depicts the complete details of the Flat areas and Sttep areas. In Flat areas, there are 345 no. of nodes and 535 no. of pipes with a total of 190 subcatchments and 75500m in length. Moreover, it has an average pipe length of 68.78m with 520ha area, 390 ha runoff area, and 11 outlet candidates in total. This area has an elevation of 19m elevation. Under Sttep areas, there are 720 no. of nodes and 920 no. of pipes with a total 720 subcatchments and 51217m lengths. Moreover, it has an average pipe length of 56.89m with 190ha area, 120ha runoff area, and 12 outlet candidates in total. This area has got 590-560m elevation.

Table 1. Details Of Flat And Sttep Areas

	Total No. of Nodes	Total No. of pipes	Total No. of Subcatchments	Total lengths (m)	Average pipe lengths (m)	Total area (ha)	Total runoff area (ha)	Total No. of outlet candidates	Elevation (m)
Flat areas	345	535	190	75500	68.78	520	390	11	19
Sttep areas	720	920	720	51217	56.89	190	120	12	590-560

Table 2. Details Of Fully Centralized Designs

Design (Fully centralized)	LCC (M. Rials)	DC (%)	Average diameter (m/ m)	Average buried depth (m)	Maximum diameter (m)	LAI [M2]	ARI [-]
1	343822	100	0.60	2.66	2.33	125559	97.28
3	257671	59	0.52	2.23	1.83	97333	98.886
5	261131	55	0.50	2.29	1.88	103704	98.986

Table 2 represents the fully centralized outcome of the ODLSA-UDN model. Under 1 design, there are 343822 LCC with 100%DC, average diameter of 0.60m/m, and 2.66m buried depth with 2.33m diameter. It has LAI [M2] of 125559 and ARI [-] of 97.28. Moreover, under 3 design, there are 257671 LCC with 59%DC, average diameter of 0.52m/m, and 2.23m buried depth with 1.83m diameter. It has LAI [M2] of 97333 and ARI [-] of 98.886. At last, under 5 design, there are 261131 LCC with 55%DC, average diameter of 0.50m/m, and 2.29m buried depth with 1.88m diameter. It has LAI [M2] of 103704 and ARI [-] of 98.986.

Conclusion

In this article, we present an optimum DL-based scheduling process for UDNs, named the ODLSA-UDN technique. The presented ODLSA-UDN model aims for the optimal control of a 1-stage pumping station and the synchronized control between 2-stage pumping stations. In addition, the ODLSA-UDN technique applied the SE-FCN water level prediction technique of the sewage pumping areas, and then, relying on the mechanism of the drainage pipeline system analysis, the causes that can result in the water level modification of the pumping station are achieved. Additionally, the parameter tuning of the SE-FCN approach occurs using BBOA. Grey correlation analysis is implemented on these main factors, and the prediction technique is identified by considering the factors with the maximum correlation amount as input. The stimulated outcomes indicate that compared to the conventional prediction approach, the proposed method not only has greater prediction precision but also has improved inflection point tracking capability.

References

1. Aderyani, F.R. and Mousavi, S.J., 2024. Machine learning-based rainfall forecasting in real-time optimal operation of urban drainage systems. Journal of Hydrology, 645, p.132118.
2. Kwon, S.H. and Kim, J.H., 2021. Machine learning and urban drainage systems: State-of-the-art review. Water, 13(24), p.3545.
3. Zhong, Q., Situ, Z., Zhou, Q., Xiao, J., Xu, X., Feng, W., Jiang, S. and Su, J., 2024. Automatic topology and capacity generation framework for urban drainage systems with deep learning-based land use segmentation and hydrological characterization. Journal of Hydrology, 641, p.131766.
4. Jiang, L., Geng, Z., Gu, D., Guo, S., Huang, R., Cheng, H. and Zhu, K., 2023. RS-SVM machine learning approach driven by case data for selecting urban drainage network restoration scheme. Data Intelligence, 5(2), pp.413-437.
5. Ma, T., Kim, J.S., Jun, C., Moon, Y.I. and Moon, H., 2024. Optimizing urban flood management: enhancing urban drainage system efficiency under extreme rainfall events. Journal of Hydroinformatics, 26(11), pp.2704-2719.
6. He, L., Ji, S., Xin, K., Chen, Z., Chen, L., Nan, J. and Song, C., 2023. Application of deep learning in drainage systems monitoring data repair—a case study using Con-GRU model. Water, 15(8), p.1635.

7. Wu, Z., Zhou, Y. and Wang, H., 2020. Real-time prediction of the water accumulation process of urban stormy accumulation points based on deep learning. IEEE access, 8, pp.151938-151951.
8. Saneii, M., Kazemeini, A., Seilabi, S.E., Miralinaghi, M. and Labi, S., 2023. A methodology for scheduling within-day roadway work zones using deep neural networks and active learning. Computer-Aided Civil and Infrastructure Engineering, 38(9), pp.1101-1126.
9. Zhang, Y., Wang, E. and Gong, Y., 2024. A structural optimization of urban drainage systems: An optimization approach for mitigating urban floods. Water, 16(12), p.1696.
10. Pei, S., Hoang, L., Fu, G. and Butler, D., 2024. Real-time control of urban drainage systems using neuro-evolution. Journal of Environmental Management, 360, p.121133.
11. Garzón, A., Kapelan, Z., Langeveld, J. and Taormina, R., 2022. Machine learning-based surrogate modeling for urban water networks: review and future research directions. Water Resources Research, 58(5), p.e2021WR031808.
12. D'Souza, S.M., Reddy, S.N., Ramesh, S., GA, S., Sravya, M.K. and Kamalpur, V., 2025, April. Smart Urban Maintenance: A Solar-Powered Autonomous Robot for Road and Drainage Cleaning Along with Waste Management Using AI. In 2025 International Conference on Inventive Computation Technologies (ICICT) (pp. 1740-1746). IEEE.
13. Fan, C., Hou, J., Li, X., Song, G., Yang, Y., Liang, X., Zhou, Q., Imran, M., Chen, G., Wang, Z. and Lu, P., 2025. Efficient urban flood control and drainage management framework based on digital twin technology and optimization scheduling algorithm. Water Research, p.123711.
14. Cai, H., Zhao, W. and Njock, P.G.A., 2024. Multi-tier scheduling algorithm of dispatching systems for urban water logging. Smart Construction and Sustainable Cities, 2(1), p.3.
15. Situ, Z., Zhong, Q., Zhang, J., Teng, S., Ge, X., Zhou, Q. and Zhao, Z., 2025. Attention-based deep learning framework for urban flood damage and risk assessment with improved flood prediction and land use segmentation. International Journal of Disaster Risk Reduction, 116, p.105165.
16. You-Fei, Z., Wei-Jie, H., Sheng, J., Juan-Juan, Z. and Wei-Guo, Z., 2023. Design of Urban Sludge Emission Reduction Optimisation Strategy Based on Fuzzy Neural Network. Ecological Chemistry and Engineering, 30(2), pp.243-250.
17. Sun, Y., Li, Y., Xu, B., Peng, Y. and Ma, Y., 2023. Operational reliability of urban drainage systems under uncertainties. Journal of Environmental Management, 331, p.117241.
18. Lee, A.R., Woo, I., Kang, D.W., Jung, S.C., Lee, H. and Kim, N., 2020. Fully automated segmentation on brain ischemic and white matter hyperintensities lesions using semantic segmentation networks with squeeze-and-excitation blocks in MRI. Informatics in Medicine Unlocked, 21, p.100440.
19. Wang, H., Huang, S., Yin, Y. and Gu, T., 2024. Short-term load forecasting based on pelican optimization algorithm and dropout long short-term memories–fully convolutional neural network optimization. Energies, 17(23), p.6115.
20. Kumar, R.S., Meera, P.S., Lavanya, V. and Hemamalini, S., 2025. Brown bear optimized random forest model for short term solar power forecasting. Results in Engineering, 25, p.104583.
21. Zhang, M., Wan, Y., He, H., Hu, Y., Zhang, C., Nie, J., Wu, Y., Deng, K., Lei, X. and Huang, X., 2025. Research on Risk Prediction of Condiments Based on Gray Correlation Analysis–Deep Neural Networks. Journal of Food Protection, 88(1), p.100419.